Tomographic Projector: Large Scale Volumetric Display with Uniform Viewing Experiences

YOUNGJIN JO*, Seoul National University
SEUNGJAE LEE*, Seoul National University
DONGHEON YOO, Seoul National University
SUYEON CHOI, Seoul National University
DONGYEON KIM, Seoul National University
BYOUNGHO LEE, Seoul National University

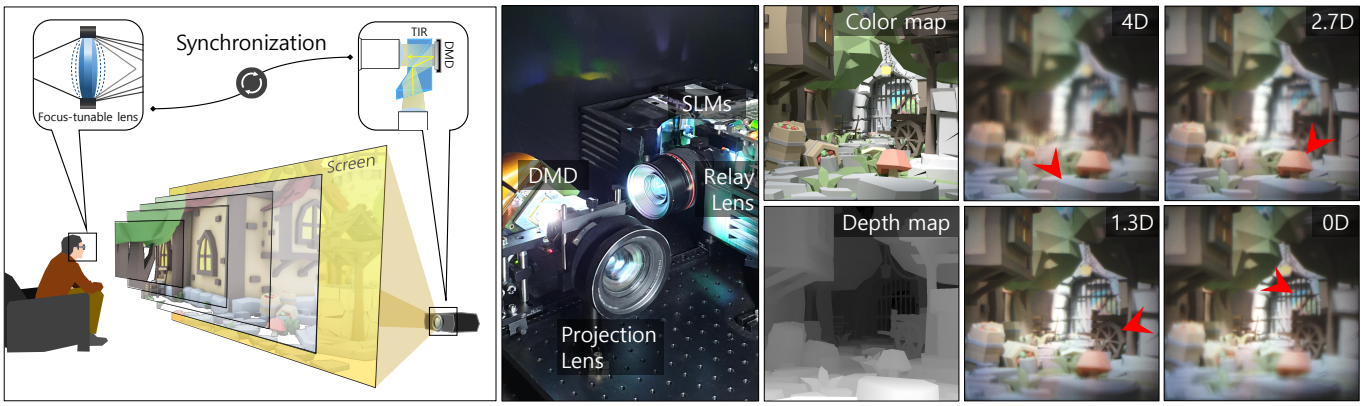

Fig. 1. Volumetric display system optimized for the use in large screen. The left side illustrates the applicable environment of the tomographic projector. The system consists of a tomographic projector that projects images onto the screen and a focus-tunable lens (FTL) located in front of the user's eye. A prototype of the tomographic projector is implemented as shown in center photograph. A projected image from spatial light modulators (SLMs) with color and contrast is relayed to digital micromirror device (DMD), and spatially filtered and projected to the screen. While the FTL modulates the focal depth of the projection screen, the DMD sequentially refreshes depth masking filters according to the depth map. Using synchronization of the DMD and the FTL for temporal-multiplexing, the tomographic projector allows a user to receive multiple depth information simultaneously. On the right hand side, we experimentally demonstrate the capability of the tomographic projector to provide focus cues.

Over the past century, as display evolved, people have demanded more realistic and immersive experiences in theaters. Here, we present a tomographic projector for a volumetric display system that accommodates large audiences while providing a uniform experience. The tomographic projector combines high-speed digital micromirror and three spatial light modulators to refresh projection images at 7200 Hz. With synchronization of the tomographic projector and wearable focus-tunable eyepieces, the presented system can reconstruct 60 focal planes for volumetric representation right in front of audiences. We demonstrate proof of concept of the proposed system by implementing a miniaturized theater environment. Experimentally, we show that this system has wide expressible depth range with focus cues from 25 cm to optical infinity with sufficient tolerance while preserving high resolution and contrast. We also confirm that the proposed system provides uniform experience in a wide range of viewing zone through simulation and experiment. Additionally, the tomographic projector has capability to equalize vergence state that varies in conventional stereoscopic 3D theater according to viewing position as well as interpupillary distance. This study is concluded with thorough discussion about tomographic projectors in terms of challenges and research issues.

CCS Concepts: • **Computing methodologies** → *Virtual reality*; • **Hardware** → *Displays and imagers*; *Emerging architectures*;

Additional Key Words and Phrases: Stereoscopic Displays, Focus Cues, Large Scale 3D Displays

ACM Reference format:
YOUNGJIN JO, SEUNGJAE LEE, DONGHEON YOO, SUYEON CHOI, DONGYEON KIM, and BYOUNGHO LEE. 2019. Tomographic Projector: Large Scale Volumetric Display with Uniform Viewing Experiences. *ACM Trans. Graph.* 38, 6, Article 215 (November 2019), 13 pages.
https://doi.org/10.1145/3355089.3356577

*Both authors contributed equally to the paper

0730-0301/2019/11-ART215 $15.00
https://doi.org/10.1145/3355089.3356577

1 INTRODUCTION

From the silent film era to the current 3D cinema, movie theaters have been continuously developed to provide audiences with more realistic and immersive experience. Recently, stereoscopic 3D movies

were introduced in most theaters where audiences can perceive depth information of imagery. Stereoscopic 3D movies allow audiences' two eyes to observe different images with binocular disparity [Mendiburu 2012]. With the physiological stimulation, stereoscopic 3D movies could deliver unprecedented immersive and realistic viewing experience. Stereoscopic 3D movie industry has already proved its commercial value, notwithstanding discomfort involved by wearing glasses for stereoscopic observation. In 2009, we witnessed a tremendous success of 3D movie 'Avatar', which is still ranked as one of the most profitable movies. However, several concerns have been reported since stereoscopic 3D movie was commercialized. Some people had uncomfortable experiences such as dizziness and nausea after watching a stereoscopic 3D movie [Nojiri et al. 2004].

One of the most convincing causes of those uncomfortable experiences is visual fatigue [Lambooij et al. 2007]. Visual fatigue comes from the discrepancy between observing a stereoscopic 3D imagery and a real volumetric object. When we perceive an object, human vision system obtains 3D information based on binocular disparity and monocular focus cues. However, most stereoscopic 3D systems are only capable to provide binocular disparity among those two depth cues. The absence of monocular focus cues may cause visual fatigue in some circumstances [Kooi and Toet 2004]. In that case, viewers unconsciously confuse because the depth information corresponding to the binocular stimulation is different from that of monocular focus cue. In stereoscopic 3D theaters, binocular images stimulate the two eyes to converge on various depths to feel 3D effect. However, the monocular focus cue is fixed at the screen depth where eye-lenses should focus for clear observation. When attempting to perceive an object with a different depth from the screen, viewers may experience a conflict between vergence and accommodation. If this conflict is significant, viewers recognize double images or blurred screen images. This is called vergence-accommodation conflict [Hoffman et al. 2008], which should be mitigated for comfortable viewing by providing adequate focus cues.

To provide focus cues in 3D theaters, we need to consider and satisfy various challenging requirements. First, the display system should have sufficiently high angular resolution so that human visual system can make focused images of virtual scene. Second, it is necessary to ensure that every audience has the equal viewing experience regardless of seat location. Third, the display system should have large viewing zone to accommodate many audiences. Although several researches have been introduced to improve 3D theater experience, none of them satisfies the three conditions because they mostly aimed to realize glasses-free environment. For instance, super multi-view display [Takaki and Nago 2010] and integral imaging display system [Park et al. 2014] sacrifice spatial resolution to increase angular resolution and duplicate binocular images. Holographic projector [Wakunami et al. 2016] has fixed viewing position, which is not appropriate in the theater environment where providing wide viewing zone is a valuable factor.

Here, we conceive a tomographic projection system that allows audiences to obtain focus cues as well as binocular disparity. The proposed system has various advantages: provide a wide range of focus cues without a loss in the expression range of resolution, frame rate, and bit depth; allow every audience to have the similar viewing experience; and secure a wide viewing zone that accommodates many viewers. These significant performances are realized by a conceptual shift that adopts wearing stereoscopic glasses. In the tomographic projection system, every audience is supposed to wear a pair of focus-tunable lenses. Inspired by tomographic near-eye display system [Lee et al. 2019], the focus-tunable lenses are synchronized with a tomographic projector to reproduce multiple focal planes via temporal multiplexing. While FTL rapidly changes the depth of a projection screen, the tomographic projector introduces appropriate images to the screen. At the same time, the binocular disparity could be achieved by applying either of shutter glasses or polarization glasses. The tomographic projector consists of a digital micromirror device and liquid crystal panels to refresh screen images at the fast frame rate.

The tomographic projector can be considered as a volumetric display with multiple planes placed in wide depth range so that it greatly enlarges the range of expression of 3D contents. Our projection system enables users to view close objects in stereoscopic 3D without VAC and provides more immersive 3D experience. In addition, the proposed system can alleviate the distortion problem caused by the difference in eye separation of each person in conventional stereoscopic 3D. Moreover, adding a DMD to an optical structure of an ordinary projector is industry-wise feasible. In this study, we first look at the principle and background of the proposed system and demonstrate the capability of the tomographic projector to form adequate focal planes. Second, we thoroughly analyze geometric specifications of our system in terms of viewing distance, viewing angle, and eye-box. Third, an optimization algorithm is introduced to enlarge eye-box of synthesized scenes and present accurate occlusion boundary without noticeable artifacts. We conclude with the discussion of the future works to improve the experiences with tomographic projection system. Specific contributions are as follows:

- We propose a projection type volumetric display that can be applied to a large screen such as a movie theater.
- We verify that tomographic projector supports continuous focus cues, preserved resolution and wide viewing zone.
- We demonstrate that proposed system allows audiences to obtain extended depth range in stereoscopic 3D.
- We introduce an optimization algorithm to enlarge eye-box and mitigate artifacts at the occlusion boundary.
- We show that tomographic projection system could mitigate the vergence accommodation conflict that arises in stereoscopic 3D.

2 RELATED WORKS

2.1 Stereoscopic 3D for Large Scale

It has been an interesting research topic to improve viewing experience of 3D theaters. Several approaches have been introduced to allow audience to have more comfortable or immersive experience. One of these efforts is to make viewing condition convenient by eliminating the need for special glasses [Dodgson 2005]. From the integral imaging [Lippmann 1908] proposed by G. Lippmann in 1908 to the compressive light field [Wetzstein et al. 2011], it has

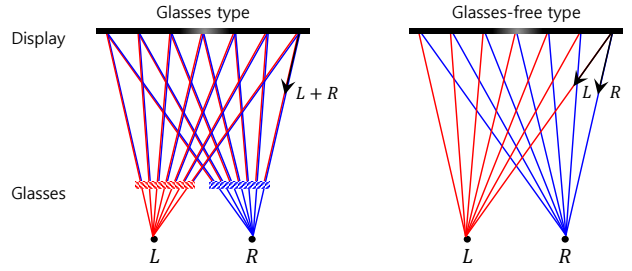

Fig. 2. Illustration of stereoscopic 3D displays with or without glasses. Both systems deliver depth information via binocular disparity. Compared to glasses type displays, glasses-free type displays should reconstruct light field or holographic wavefront to provide binocular disparity.

been researched steadily. For the binocular disparity in glasses-free system, different information should be provided for each direction as shown in Figure 2. To achieve this, methods for forming an angular resolution through the barrier [Choi et al. 2008; Peterka et al. 2008], lenses [Kim et al. 2007; Park et al. 2009], stacking of panels [Isono et al. 1993; Lanman et al. 2010] , and interference of light [Li et al. 2016; Wakunami et al. 2016] have been proposed. However, the information that the display can generate is limited by the spatial resolution, and in order to produce the angular resolution, a reduction in the spatial resolution is inevitable. Thus, autostereoscopic displays cannot be directly implemented in a wide cinema setting without the trade-off relation.

The efforts have been made to relieve the trade-off and increase the number of viewpoints by using multiple displays or applying temporal multiplexing techniques. Recently, various methods have been proposed to reduce the cost of spatial or angular resolutions. One of them is to provide replicated viewing zone to the entire audience [Efrat et al. 2016]. This method use an optical construction based on parallax barriers to replicate the narrow range contents to all seats. In another method, a projection system using compressive light field [Hirsch et al. 2014] was implemented, which reconstructs light field by projecting a multi-layered display on a lenticular-based screen. Their light-field projection system adopts a computational approach to compress light field so that the viewing range is improved through angle expanding screen.

All of the above solutions aimed to provide more comfortable viewing experience by eliminating the need for glasses. In 3D theater, however, giving immersive experiences is just as important as comfort. Many researches have been conducted on various ways to enhance visual experiences. For example, a new concept of multi-projection techniques called ScreenX was introduced [Lee et al. 2016]. In order to provide immersive viewing experiences in movie theaters, it considers the left and right side walls that work with the front screen. As part of the efforts to improve viewing experience, we propose a novel system increasing the expressible depth range of 3D contents without VAC problem. It can be a solution for immersive experiences in large scale stereoscopic 3D.

2.2 3D Displays with Focus Cues

The importance of monocular focus cues has been consistently emphasized in many research articles. Especially, providing monocular cues has been thoroughly discussed in some applications such as augmented reality (AR) or virtual reality (VR) where viewers interact with closer objects. Since the most promising display platform for AR/VR is near-eye displays that deliver the depth information mostly by binocular disparity, focus cue is important to alleviate VAC problem. To investigate how VAC affects user experience, perceptual studies based on human study have been demonstrated by various research groups [MacKenzie et al. 2010; Mauderer et al. 2014]. According to those perceptual studies, human may feel discomfort if vergence and accommodation mismatch occurs more than 0.5 diopter in an unusual way, such as stereoscopic 3D.

To mitigate VAC problem in near-eye displays, various approaches have been introduced and analyzed. First, we can implement near-eye displays that can provide focus cues: varifocal displays [Dunn et al. 2017; Konrad et al. 2016; Padmanaban et al. 2017], multi-plane/volumetric displays [Akeley et al. 2004; Chang et al. 2018; Lee et al. 2018; Narain et al. 2015; Rathinavel et al. 2018], tensor displays [Huang et al. 2015; Lanman and Luebke 2013; Maimone and Fuchs 2013], holographic displays [Jang et al. 2018; Maimone et al. 2017], and tomographic displays [Lee et al. 2019]. Each approach has different theoretical background and distinct advantages in terms of resolution, field of view, depth of field, or form factor. Second, accommodation-invariant displays [Konrad et al. 2017; von Waldkirch et al. 2003] could be another candidate for VAC mitigation. Obscuring focus cues by providing constant experience regardless of eye's focal length, accommodation-invariant displays ensure that vergence cues lead corresponding accommodation without conflict.

2.3 Comparison of Related Works

As described above, we have been observing various methodologies to provide focus cues for near-eye displays. Inspired by previous researches using DMD projectors [Chang et al. 2018; Rathinavel et al. 2018], we conceive tomographic projector that can be applied for large scale volumetric displays. Our projection system has a similar optical configuration with that of those two works. First, we equally adopt the DMD synchronized with focus-tunable lens to generate dense focal planes that are difficult to implement with SLMs. At this point, the DMD operates in a binary on/off mode, so the system requires 24-bit depth for representation of 8-bit images with full color. The prototypes of two research groups suffer from some losses in terms of bit depth or frame rate. In the case of [Chang et al. 2018], the prototype implements 8-bit gray image with 40 focal planes at 40 Hz, which is insufficient bit depth and frame rate. And for the prototype of [Rathinavel et al. 2018], it achieves 8-bit full color image with 280 focal planes at 60 Hz by using a high dynamic range (HDR) light source. In this case, because each focal plane is represented by the combination of at least 24 binary planes, the bit depth is limited at high spatial frequency [Lee et al. 2019].

In tomographic projector, we adopt additional SLMs that can represent 8-bit images with full color, giving degree of freedom to the system. It is minor modification but gives significant improvement in display performance. The proposed system can represent the

high-resolution images of the SLMs while the depth information is supported by the DMD. In addition, the SLMs can support 8-bit depth with full color expression, allowing the DMD to display a sufficient number of focal planes without making sacrifices in the spatial frequency and frame rate. However, there is the drawback that is correlation of each focal plane images, which requires a different optimization strategy to compensate for occlusion boundary artifacts. In this study, we will demonstrate convincing performance, introduce an optimization method, and thoroughly analyze the requisites for 3D theaters with focus cues.

3 TOMOGRAPHIC PROJECTOR

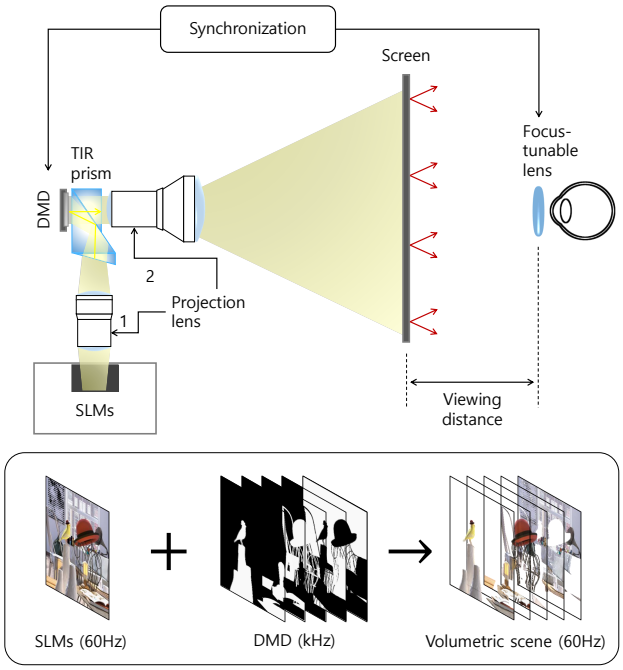

Fig. 3. Illustration of the tomographic projection system. The system is divided into a tomographic projector, a projection screen, and focus-tunable lenses. Combining SLMs and a DMD, the tomographic projector may refresh projection images at fast frame rate. Each audience is supposed to wear focus-tunable lenses synchronized with the tomographic projector. As a result, volumetric scene can be perceived by users as shown in the bottom row.

Figure 3 illustrates a schematic diagram of tomographic projector. We adopt a focus-tunable lens as an eyepiece that can sweep a wide dioptric range at the speed of 60 Hz. Through the eyepiece, the optical distance between audience and the screen changes periodically from near to far and far to near. During the single periodic cycle, the tomographic projector introduces depth-sliced sequential images onto the screen at each appropriate moment. Human vision system recognizes the sequential images at different depths as a synthesized volumetric scene because the periodic cycle of FTL takes a short time. Namely, tomographic projector is a temporal multiplexed volumetric display where the user perceives multi-focal plane images as integration of time sequential retinal images during the specific rate [Kalloniatis and Luu 2007].

Depth-sliced sequential images can be rendered by splitting the perspective image according to the depth of a volumetric scene. Adequate focus cues are delivered when tomographic projector is synchronized with the FTL to float each depth-sliced image at the desired depth. In other words, tomographic projector should have much higher refresh rate than 60 Hz to display a depth-sliced image at the desired moment. To achieve such a fast refresh rate, we combine DMD and three amplitude spatial light modulators. The combination enables much higher refresh rates while maintaining resolution and bit depth. Performing a role of localized and binarized filtering SLM pixels, DMD converts SLM images into sequential images at faster frame rate. Since DMD is possible to operate at 16 kHz, it has the capability to refresh projection images more than 260 times within 1/60 second [Rathinavel et al. 2018]. Note that the resolution and bit depth of projection images are determined by SLMs' specifications.

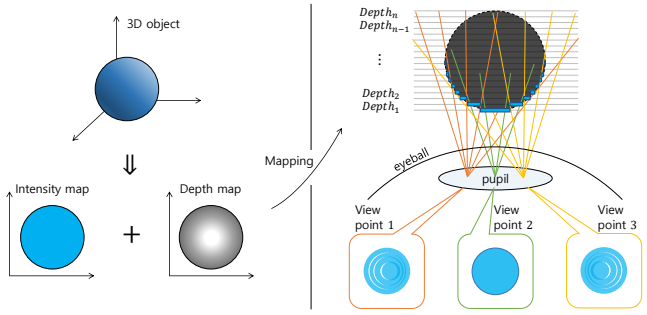

Fig. 4. Depth-sliced decomposition of volumetric scene when an intensity and depth map are provided. Although each voxel is allocated at accurate focal depths, it is not guaranteed that viewing experience is immersive and realistic. As illustrated in right hand side, synthesized view images may contain artifacts such as separation or overlap according to the view points within the eye-box.

As each depth-sliced image is optically floated at corresponding distance through the FTL, the audience is expected to have comfortable experience without VAC. However, it does not guarantee immersive experience because of the difference between a synthesized scene and the actual scene. Compared to the real environment, each depth-sliced image of tomographic projector cannot conceal light from a rear plane. As illustrated in Figure 4, the limitation results in artifacts that are usually observed in the area where the depth discontinuity is significant. To mitigate the artifacts, alternative rendering approaches have been introduced in various researches that have similar limitation. It has been verified that occlusion of light field can be imitated by optimizing multi-focal plane images [Narain et al. 2015]. Inspired by this idea, we could alleviate the artifacts by optimizing DMD image sequences as well as SLM image.

The optimization of DMD sequence is similar with the reconstruction process of discrete computed tomography (DCT) [Herman and Kuba 2012]. For reconstruction of tomographic images, DCT collects X-ray illumination intensity profiles of a volumetric tissue from a few directions. The logarithm of an intensity profile is given by line integral of attenuation coefficient. The volumetric profile of attenuation coefficient can be reconstructed by back projection of the

intensity profiles. As a result, DCT reconstructs low bit depth (e.g. binary) tomographic images that represent volumetric information of the tissue. In tomographic projector, the logarithm of an X-ray intensity profile corresponds to a perspective view image within the eye-box. The binary tomographic images correspond to the DMD image sequences. Therefore, we could optimize DMD image sequence for optimal representation of volumetric scenes via similar approach of tomographic reconstruction. Details of optimization procedure are demonstrated in Section 5.2.1.

4 IMPLEMENTATION

4.1 Miniaturized Tomographic Projection System

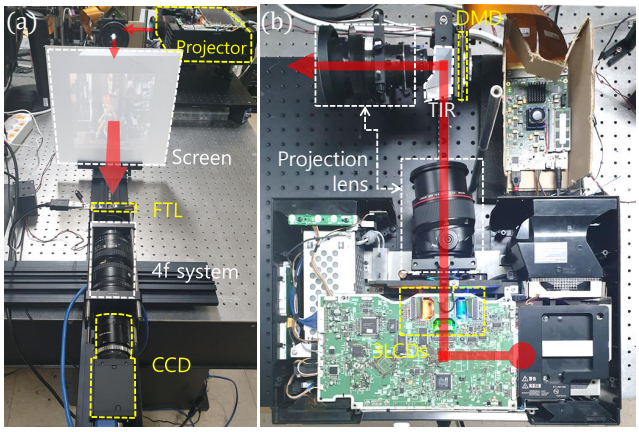

Fig. 5. Photograph of (a) the prototype projection system and (b) the tomographic projector. 4f relay optics are supplemented between a FTL and a CCD camera to adjust eye relief regardless of the camera lens size. Note that our prototype is a 25 times miniaturized version of 3D theater.

To investigate the feasibility of tomographic projector and demonstrate the seating capacity in theater environment, experimental setup is built as shown in Figure 5. Tomographic projection system consists of a set of three SLMs representing RGB image, a DMD with a total internal reflection (TIR) prism, projection lens units, and a focus-tunable lens located in front of the eye. In detail, an RGB image formed by the projector is relayed to DMD through the first projection lens and total internal reflection prism. Then, DMD locally filters the RGB image to refresh projection images 60 times within 1/60 second. Passing through the second projection lens, the filtered images are introduced to the screen. Each sequential screen image is shown to the user at the intended depths by the FTL that periodically tunes its focal length with synchronized DMD. The FTL sweeps the depth of a virtual screen along the depth range between 25 cm (4 D) and infinity (0 D) at 60 Hz. The depth range is represented by 60 focal planes those interval is 0.07 D. Accordingly, the user can perceive 60 focal plane images simultaneously.

Figure 6 demonstrates the result of tomographic projector prototype. A volumetric scene is along the depth range between 0 D and 4 D. As shown in the results, the depth information of 3D contents is well provided while preserving high resolution and contrast. Projection image has a resolution of 670×670 with a frame rate of 60

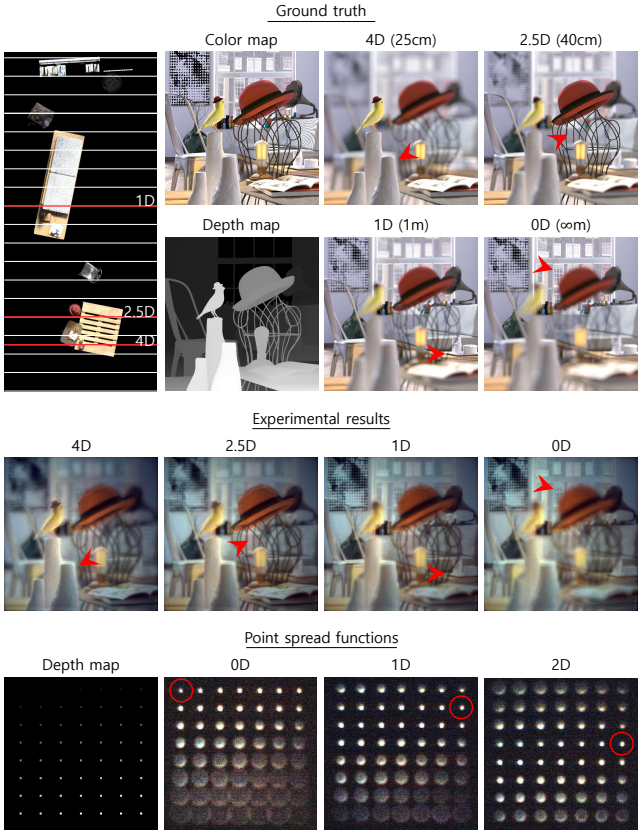

Fig. 6. Experimental results to demonstrate the feasibility of tomographic projector. On the left, perspective view image and corresponding depth map are illustrated with a top view of target volumetric scene (Source image courtesy: "InteriorScene" www.cgtrader.com). To demonstrate the ability of tomographic projectors to provide focus cues, we captured reconstructed images according to the CCD camera's focal depth. As shown in photographs, the target volumetric scenes are reconstructed with quasi-continuous focus cues (top). We also captured point-spread functions in different focal planes at the rate of 60 hz (bottom). The distance of the points gradually decreases from the upper left to the lower right. The red arrows and circles indicate in-focus areas.

Hz. Through the changes in point-spread function, we confirm that multifocal planes are well formed. Assuming eye relief, the distance from the eye to FTL, is 14 mm, system has the diagonal field of view (FOV) of 39 degrees limited by the aperture of FTL. The projector screen is at 40 cm away from FTL and the image size is 20 cm. Note that the system can reproduce on a larger scale but is limited by the experimental space. This can be considered as an environment where the size of theater is reduced by 25 times or more. In this case, it is a theater environment that can accommodate up to 91 people (8 m×6.6 m). We believe the experimental results could be extended to the original scale environment without significant or unexpected artifacts. System resolution, occlusion artifacts and focus cues are not expected to be changed from the scaled down results.

4.2 Hardware

PT-AE1000E beam projector is disassembled and modified for three SLMs to represent RGB image. RGB image is relayed to the DMD by using a tilt-shift lens (Canon TS-E 80mm) because the micromirror of the DMD has a tilt angle of 12° between on- and off-state and the illumination should be done 24° (2X the tilt angle) from the vertical. The tilt shift lens allows the image planes to be slanted according to the Scheimpflug principle which refers to the relationship between the image plane and a tilted imaging lens in geometrical optics [Larmore 1965]. DLP9500 from Texas Instrument is employed as the DMD which has FHD resolution (1920×1080). Since the illumination should enter the DMD at 45 degrees (perpendicular to the micromirror hinge-axis), We only use a resolution of 720×720 rotated 45 degrees as the spatial modulation area.

Focus-tunable lens used in the experiment is EL10-30-TC-VIS-12D of Optotune. FTL can sweep the focal length from 50 mm to 180 mm at 60 Hz. A negative offset lens is integrated in front of FTL to drop the focus sweep range to a negative number. This makes FTL possible to express an object closer than screen. The focal length of offset lens is -75 mm, and shifted focal range is between -5 D and 6.7 D. Because the screen is 400 mm away in experimental setup, FTL diopter should sweep the range between -1.5 D and 2.5 D to represent 4 D. We adopt 4f relay in front of CCD camera using lenses with a f-number of 1.4 (Nikon). It is to secure the eye relief limited by C-mount lens. For synchronization of FTL and DMD to display the images at an intended depth/an appropriate time, we use the data acquisition (DAQ) board from National Instrument. The DAQ board generates two reference clock signals that are synchronized by using LabView. One is the triangle wave at 60 Hz varying the focal length of the focus-tunable lens. The other one is for DMD to update the sequential backlight images. It is the square wave at 7200 Hz for 60 focal planes. A detail description of the synchronization is provided in Supplementary Material.

5 ANALYSIS

5.1 Determine Viewing Zone with Uniform Experience

One of the most important goals of 3D theater is to deliver uniform 3D experience regardless of viewing position. In stereoscopic 3D theaters, audiences perceive distorted depth cues due to geometric difference in viewing position, such as distance from the screen and angle from the normal perspective view. Similarly, the depth information provided by tomographic projector could also be distorted when the viewing position changes as shown in Figure 7. The depth distortion of 3D contents may result in an inconvenient experience. The following section analyzes the relationship between depth distortion and viewing position based on geometric analysis of tomographic projector.

5.1.1 Geometric Analysis in Spherical Coordinate. In tomographic projector, each focal plane depth is determined by the focal length of FTL according to the thin lens formula below.

$$1/d_o + 1/(-d_i) = 1/f, \tag{1}$$

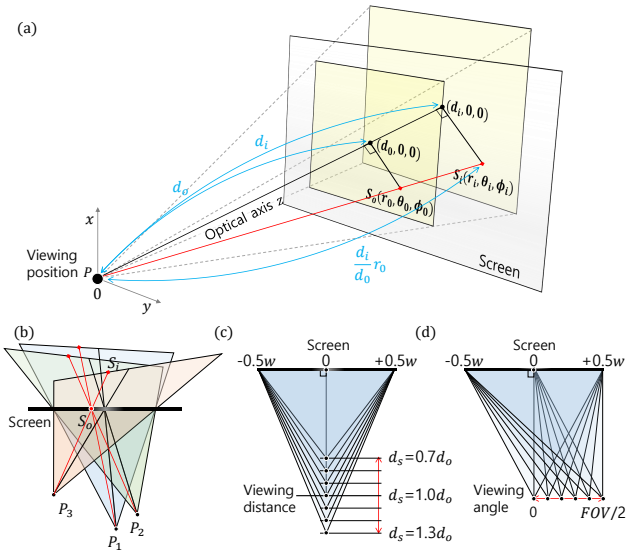

Fig. 7. Illustration of the geometric distortion analysis. In spherical coordinate system, the virtual image magnified by a lens is formed in the same direction (a). At this time, the depth information of the virtual image would be different depending on the viewing position (b). The degree of geometric distortion varies according to the (c) viewing distance and (d) viewing angle.

where o is the distance to a screen and f is the focal length of FTL, the distance $i > 0$ of virtual image can be calculated.

$$M = d_i/d_o. \tag{2}$$

The magnification ratio M of virtual image is proportional to the floating distance i. When there is a pixel of S_o as shown in Figure 7 (a), it will be magnified by the lens and placed at S_i. In the spherical coordinate, S_i can be expressed as following principle of similar triangles.

$$r_i = Mr_o, \theta_i = \theta_o, \phi_i = \phi_o \tag{3}$$

where r, θ, and ϕ are spherical coordinates where the origin is the center of FTL. As shown in the equation, θ and ϕ are constant regardless of the magnification ratio. In other words, there is no angular movement of the pixel while the focal length of FTL varies. Note that it is valid regardless of optical axis direction or central position of FTL.

5.1.2 Viewing Distance. According to the Eq. 1, the virtual screen depth is related to the focal length of FTL, but also viewing distance d_o. If the viewing distance is shifted from the reference value, focus cues will be distorted. Figure 8 (a) and (b) illustrate how viewing distance change accumulates the focus cue error. The focus cue error caused by changing the viewing position is given by

$$D_{err} = |1/d_s - 1/d_o|, \tag{4}$$

where d_o is the reference viewing distance to the screen and d_s is the changed viewing distance. We confirm that the depth distortion occurs in the experimental environment where most specifications are 25 times miniaturized.

In a practical sense, however, the depth distortion caused by viewing distance variation is negligible by following reasons. First,

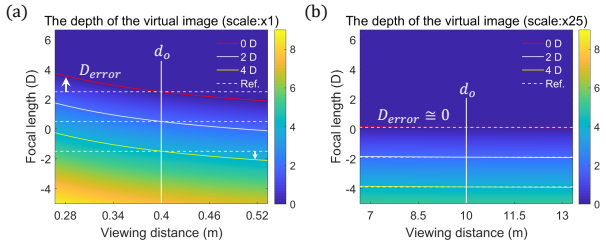

Fig. 8. The simulation results of focus cue error when the viewing distance is changed by ±33%. The color bar refers to the focal depth of screen. The red and yellow lines indicate the conditions where focal depths are constant at 0 D and 4 D respectively. (a) In laboratory setting, shifted focus cues are provided when viewing distance is adjusted from the reference at d_0. Compared to white dashed line that indicates desired performance, focus cues provided by tomographic projection system may contain dioptric errors. (b) In 25 times scale-up environment, however, stimulated focus cues follow the guide line regardless of viewing distance.

the variation of viewing distance becomes much less influential in the actual theater environment where the scale of the system is increased (25 times larger). This is because the focus cue error is proportional to the reciprocal of the reference viewing distance as shown in Eq. 4. Second, severe depth variation can be corrected by adjusting sweep range of FTL or the focal length of the offset lens. Since the optical power of FTL increases with current linearly, the change of the sweep range can be controlled by shifting the offset value of the input signal (white line in Figure 8). Third, this focus cue error is usually much smaller than the binocular depth distortion that occur in a conventional stereoscopic 3D.

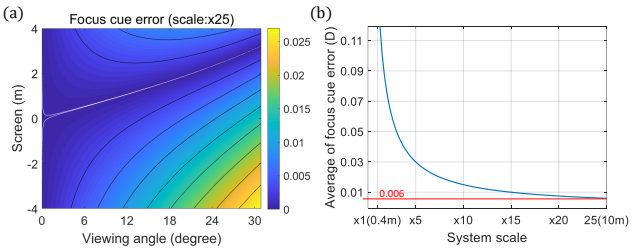

Fig. 9. (a) Focus cue error analysis when the viewing angle shifts up to 31° in 25 times scale-up environment. The color bar refers to the focal depth of screen. Similar to viewing distance analysis, (b) the degree of focus cue error caused by viewing angle shift is also in inverse proportion to the reference viewing distance.

5.1.3 Viewing Angle. Most theaters could not accommodate every audience in the central seat. Some of audiences should watch the screen from different slanted vertical or horizontal angles. However, variation of viewing angle may lead to the depth distortion in tomographic projector. It occurs because the optical axis of the lens is not always perpendicular to the screen when the viewing angle varies. In other words, the virtual screen image becomes slanted according to the viewing angle. This phenomenon causes focus cue error that can be expressed as follows.

$$D_{err} = |1/(d_s \sec\theta - x \sin\theta) - 1/d_s|, \tag{5}$$

where θ is the angle from the normal perspective view and x is the displacement away from the center on the screen. Note that we assume that the optical axis of FTL is toward the center of the screen.

The simulation results in Figure 9 show focus cue error caused by viewing angle variation. While changing the viewing angle up to 30.9 degree which is the half FOV of the closest seat based on SMPTE standard, we calculate the degree of focus cue error in the horizontal direction of the screen. In the experimental environment, the depth distortion of up to 0.5 D is observed. In contrast to viewing distance dependent focus cue error that can be compensated by modulation of FTL, it is difficult to correct viewing angle dependent focus cue error individually. However, the distortion is decreased to negligible amount in 25 times scale-up environment as shown in Figure 9 (b). It can be also explained by the fact that the focus cue error is inversely proportional to the viewing distance. In summary, we reach the conclusion that the tomographic projector can provide the uniform 3D experience in terms of focus cues. Under the practical environment where the screen is at a distance of meters, tomographic projector has a wide viewing zone as illustrated in Figure 10.

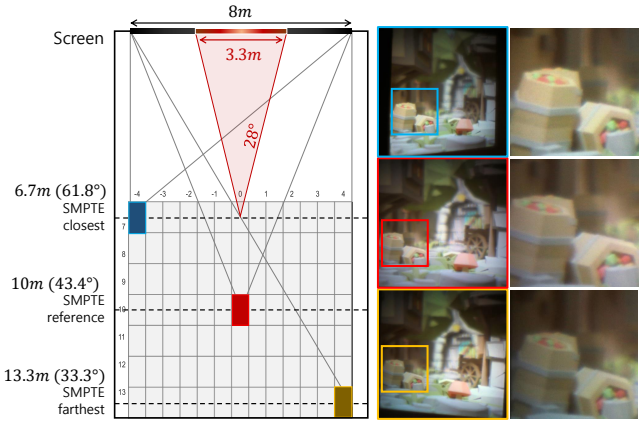

Fig. 10. Simulated viewing zone of an actual theater environment where the screen is 8 meters wide. The viewing zone is determined according to SMPTE standard EG 18-1994 which is the guideline of the horizontal viewing angle (HVA) for movie theaters, and the number of seats is 7 (row)×13 (column). Uniform viewing experiences at three seats are demonstrated by capturing photographs from corresponding position in miniaturized experimental environment.

5.1.4 Vergence-Accommodation Conflict. In previous sections, we have verified the capability of our suggested system to support accurate focus cues regardless of the viewing position in theaters. However, we should consider another term related to distortion of binocular cues according to the viewing position [Gao et al. 2018; Shibata et al. 2011], which can give rise to unexpected VAC. When a viewing distance changes from d_o to d_s, vergence distance of z_o changes to z_p as shown in Figure 11 (a). Considering it as depth range, the range users feel is inversely proportional to the distance of the screen.

$$z_p = z_o * d_s / d_o \tag{6}$$

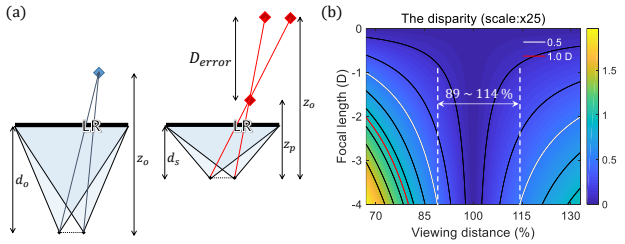

Fig. 11. Illustration of (a) vergence distance error and (b) the degree of VAC according to viewing positions. As illustrated in figure, vergence angle of two eyes to merge disparity images is dependent to the viewing position. The vergence distance error gives rise to unexpected VAC problem.

While tomographic projector provides uniform focus cues regardless of a viewer's position, vergence distance is unstable. It may give discomfort to the viewers due to VAC that is given by

$$D_{err} = |1/z_p - 1/z_o|. \tag{7}$$

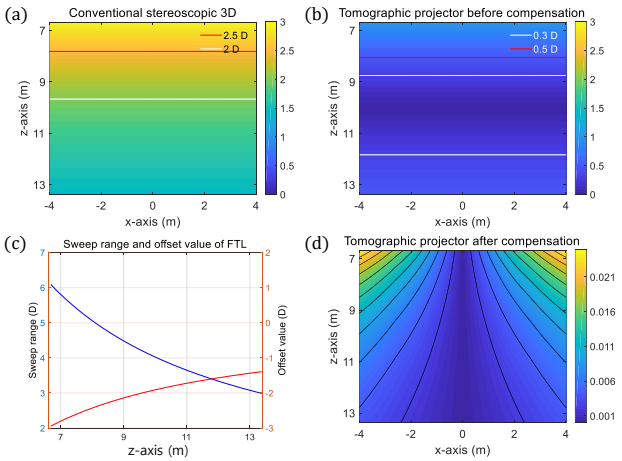

Fig. 12. The VAC analysis for (a) conventional stereoscopic 3D system and the (b) tomographic projection system when the binocular parallax is provided up to 4 D. Each color bar indicates average value of VAC in dioptric unit. (c) VAC can be further alleviated if FTL is employed for correction of the vergence error. It is done by changing the sweep range (blue line) and the offset value (red line) corresponding to each viewing distance. (d) The compensation result of VAC is represented. After the depth distortion is compensated, there is not significant VAC regardless of viewing position.

According to previous research, people with the focus cue error above 0.5 ~ 1 D would feel discomfort [Percival 1892]. Typically, a cinema screen is a few meters apart so the focus diopter is less than one. At this time, vergence distance of the contents should be larger than 1 m in order to avoid discomfort to audiences. In the case that the binocular disparity is provided as 4.0 D in the conventional stereoscopic 3D system, the disparity between vergence and accommodation distance is larger than 3.0 D so there is a severe conflict between accommodation and vergence. On the other hand, the proposed system has some comfortable viewing range as shown by the red line in Figure 12 (b). In this specification, 71 people out of 91 seats can experience a volumetric scene without VAC. Furthermore, by adjusting focus cues at each position individually as shown in Figure 12 (d), audiences may enjoy comfortable viewing experiences without any significant VAC in all seats. In summary, tomographic projection system can effectively alleviate the VAC problem according to the viewing distance compared to conventional stereoscopic 3D.

5.2 Eye-box for Individual Audience

In tomographic projection system, it is also important to analyze tolerance of individual viewing experience because a viewer wears a pair of focus-tunable lenses to see virtual images. The pair of focus-tunable lenses allow the viewer to see adequate volumetric imagery within the exit-pupil or eye-box. The exit-pupil indicates an area where scattered light from the projection screen can be delivered. The viewer's eye should be located within the exit-pupil to see the entire projection screen without the vignetting effect. The eye-box is referred to as a region where the viewer can observe accurate volumetric imagery. If the viewer's eye is located outside the eye-box, the viewer can recognize the artifacts of volumetric scenes as previously illustrated in Figure 4. Therefore, tomographic projector should secure sufficiently large exit-pupil and eye-box to have tolerance for the pupil movement.

The tomographic projector reconstructs several focal plane images that are synthesized to formulate a volumetric imagery. The alignment of focal plane images is important to reconstruct accurate volumetric scenes. However, the alignment of focal plane images varies according to the pupil position. When the pupil is dislocated from a desired point, the viewer recognizes separation or overlap of focal plane images. Accordingly, the eye-box of tomographic projection system is supposed to be limited on the fixed point. This phenomenon also involves artifacts in the representation of occlusion boundaries [Narain et al. 2015]. However, we could enlarge the eye-box by applying a computational optimization that solves a binary least squares problem. Inspired by previous researches that alleviate occlusion boundary artifacts in multi-plane displays, we conceived an algorithm to solve the least squares problem for the tomographic projector.

5.2.1 Optimization Algorithm. The binary least squares problem has similarity with least squares problems for multi-plane displays [Mercier et al. 2017; Narain et al. 2015; Xiao et al. 2018]. In multi-plane displays, we find optimal focal plane images that reconstruct accurate retinal focal stacks or pupil view images. We may apply similar approach to optimize focal plane images reconstructed by the tomographic projector. However, it is necessary to consider the distinct features of the tomographic projector. One characteristic of the tomographic projector is the correlation between focal plane images. Focal plane images of the tomographic projector are determined by the multiplication of single 24-bit image on the SLM and 1-bit images on the DMD. In other words, all focal plane images share the information given by the identical 24-bit image on the SLM. Second, we need to consider that the DMD only supports 1-bit images, which is referred to as a binary constraint of least squares problem. The binary constraint makes least squares problem non-deterministic polynomial-time hard (NP-hard).

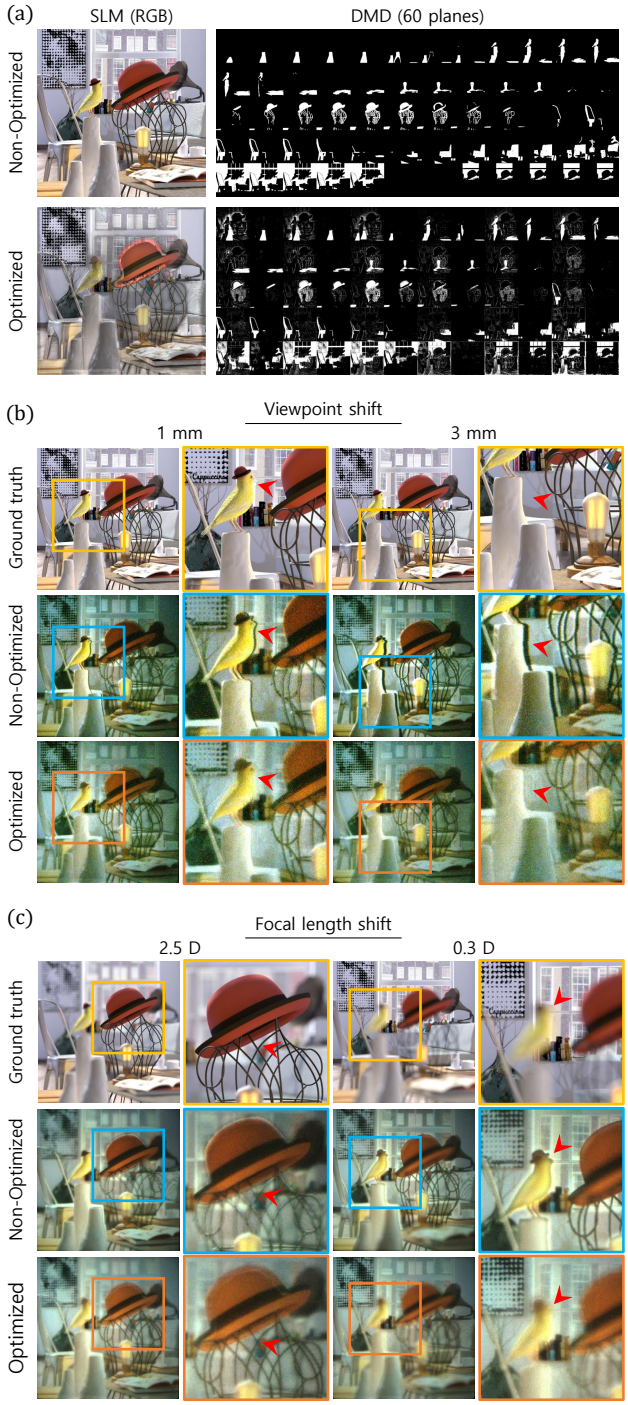

Fig. 13. Experimental result to demonstrate validity of the optimization. (a) We illustrate SLM images and DMD image sequences with and without optimization. We verify the feasibility of the optimization by changing the (b) viewpoint and (c) focal length of CCD camera. As indicated by the red arrows in results, the artifacts are mitigated using the optimization.

In this study, we solved the relaxation of the NP-hard problem by applying an alternating least-squares (ALS) strategy. We independently update the SLM image and the DMD image sequence. Each iteration consists of two least squares problems to update the SLM and DMD images. For instance, the DMD image sequence is assumed as a constant when the SLM image is updated, and vice versa. To make least squares problems easy to solve, we ignore the binary constraint for the DMD images at each iteration. Without the binary constraint, the two least squares problems can be solved by using SART [Andersen and Kak 1984]. The image sequence is initialized with the given RGB-D image, and the number of iterations is 100. Every 30 iterations, the DMD images are transformed to a binary image sequence that shows minimum errors of energy as well as variance. The energy is the sum of DMD image sequence, and the variance is the absolute difference caused by the updates. If there is a DMD pixel supposed to be 0.25 for the first three images and 0.3 for the last image, the corresponding binary image pixel becomes 1 for the last image to balance the energy (i.e. 1.05).

5.2.2 Motion Parallax and Adequate Focal Blur. To provide accurate motion parallax and enlarge the eye-box size, we need to reconstruct four-dimensional light field introduced to the pupil plane. Accordingly, perspective view images on the pupil plane are used as a target for the optimization [Huang et al. 2015]. In the optimization, SLM and DMD images are updated to minimize the errors between the ground truth and reconstructed pupil view images. Figure 13 (a) demonstrates the optimized SLM image and DMD image sequences. When these images are applied for the tomographic projection, separation or overlap of focal plane images is alleviated when the viewer's pupil moves as shown in Figure 13 (b). In other words, the tolerance for the pupil movement and the eye-box size are increased. Additionally, we may see that the occlusion boundary artifact is also mitigated because the pupil view images are reconstructed with an enough accuracy. As can be seen from the result, the presented optimization algorithm allows the tomographic projection to be improved in terms of fidelity and tolerance.

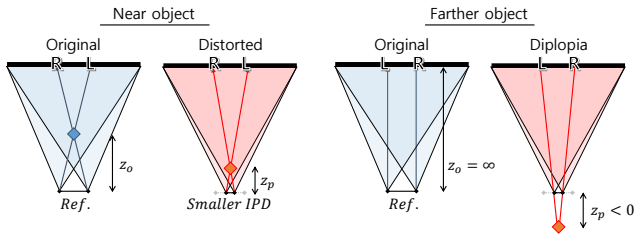

Fig. 14. Vergence cue distortion caused by IPD variation. When IPD is smaller than reference, the user experiences exaggerated 3D than the ground truth. An object in front of the screen gets closer, and another object beyond the screen gets farther. The binocular disparity of the screen larger than IPD causes diplopia for the farther object.

5.2.3 Tolerance for Interpupillary Distance Variation. Eye separation (interpupillary distance, IPD) should be considered importantly when creating 3D content production. Generally, it has a value of around 63 mm, but there is a deviation for each person. If a user has an IPD that differs from the value used when creating 3D content, a

depth distortion will be happened while watching. Especially when it is smaller than the reference IPD, the eyes can be diverged from the center to the outside and viewers may perceive double vision (diplopia) without convergence. This ocular divergence can occur in people with a smaller IPD such as children and women, which causes visual fatigue [Ukai and Howarth 2008].

If the tolerance of the eye-box is increased by applying the optimization, it is possible to compensate various IPD per user. In other words, the proposed system could solve the IPD mismatch caused by human variation in conventional stereoscopic 3D. It can be achieved by making the interspace between the focus-tunable lenses the same as the reference. In this case, since the focus cues are adjusted optically as much as users' IPD deviates from the reference, the distortion can be compensated within the eye-box of the system.

6 DISCUSSION

6.1 Compensation of Vergence Distortion

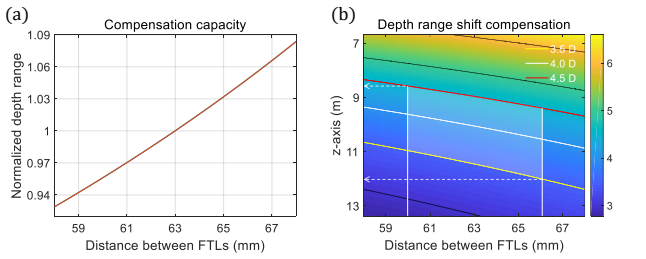

Fig. 15. Simulation results of the compensation by changing the interspace between FTLs. (a) shows the value of normalized depth range that users perceive. We consider the reference IPD as 63 mm. In that case, the boundary compensating the vergence distortion is represented at (b). The scale bar indicates the depth range.

As demonstrated in previous section 5.1.4, Stereoscopic 3D theaters provide different vergence stimulation according to the viewing position. For uniform 3D experience, it is necessary to alleviate the vergence distortion. Inspired by the fact that IPD influences the vergence distance, we conceive a methodology to compensate the vergence distortion caused by the viewing distance. If the interspace between FTLs is deviated from the reference IPD, another vergence distortion occurs. Those two different vergence distortions can be canceled in the adequate condition. For instance, an audience who experiences more exaggerated 3D because of sitting close to the screen can wear FTLs separated by smaller distance to mitigate it. Using the compensation method, the viewing zone can be extended where uniform vergence is stimulated as shown in Figure 15 (b).

6.2 Advanced system

Our projection system provides focus cues by combining three SLMs for full color 8-bit depth images and DMD in charge of local filtering. The biggest advantage of this system is that it doesn't have critical trade-offs when providing focus cues to users in different positions. However, there can be degradation in resolution due to aberration that occurs when relaying SLMs to the DMD. Since DMD consists of array of tilted mirrors, there should be an oblique incidence using TIR. For the oblique incidence, the relay lens was tilted according to

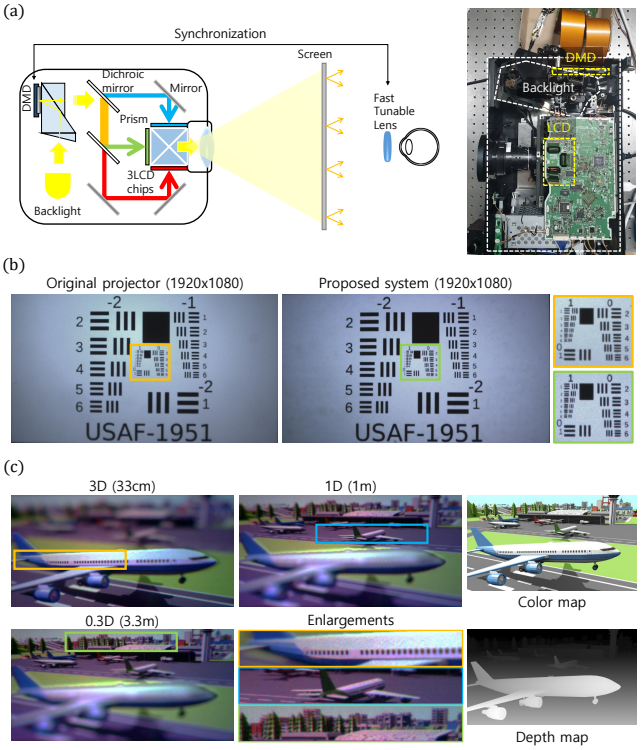

Fig. 16. (a) Schematic diagram and implemented prototype of a tomographic projector that employs DMD as a backlight instead of a filter. Experimental results of the (b) resolution target (USAF 1951) for comparison with original projector and (c) volumetric scene (Source image courtesy: "SimplePoly Urban", www.cgtrader.com).

the Scheimpflug principle in order to make the focal plane identical to the DMD plane. Although it leads the optical axis to be tilted, off-axis aberration occurs so that the resolution is degraded.

It can be improved by changing systematic strategy. Our suggestion is to insert DMD inside the projector and spatially modulate the backlight as shown in Figure 16 (a). Specifically, the light coming from a projector's lamp converges to DMD in even brightness through an integrator. This spatially modulated backlight is relayed to the three SLMs and passes through a projection lens to the screen. Implementing a prototype using this method, we confirmed that the resoultion of images is comparable to that of commercial projectors as shown in Figure 16 (b). Note that we display the white image on the DMD with a static focal length to check the spatial resolution of SLMs. In that case, the resolution of DMD's active area is 432×768 but can be improved by changing the optical system in the projector. However, there is an issue that DMD image in the red color is flipped because of the 4f lens placed in order to compensate the difference of the optical path among colors. We believe this problem would be easily solved by adjusting optical path and elements between each color. Figure 16 (c) shows the results of combining RGB images taken separately. Appropriate focus cues are provided with the original resolution of the projector.

We also believe that rearranging SLMs and DMD could better cope with brightness loss when enlarged to real environment size.

Our system has additional brightness loss caused by limited duty cycle of DMD projection. The brightness of the optimal duty cycle found by the optimization method is about 0.3 [Choi et al. 2019]. This means that the backlight unit should be three times brighter than conventional one, and this can limit the system size. However, if backlight first meets DMD that is likely more tolerant for thermal and then passes SLMs, it would be feasible to increase backlight brightness enough.

6.3 Improvement in the Focus-Tunable Lens

There are several methods to change the focal length [Stevens et al. 2018]. The focus-tunable lens used in the experiment adopts shape-changing method based on a combination of optical fluids and a polymer membrane. It is a precision product with operating speed of 60 Hz with a suitable form factor. However, diagonal field of view is calculated as 39 degrees when aperture is 10 mm and the eye-relief is 14 mm. In this case, it can only cover the farthest range from the SMPTE standard. The aperture of focus-tunable lens can be the bottle neck in the theater environment where wide range of visibility is important. Among commercial products, there is a focus-tunable lens with aperture of 16 mm from Optotune. It has a wide diagonal FOV of 59 degrees, but can cause a flicker because its operating speed is 50 Hz. With the technological development, we believe focus-tunable lens will reach a larger aperture that covers the entire field of view in near future.

In addition, for practical use, the mechanical problems occurring during the operation of focus-tunable lens need to be improved. During the synchronization, FTL has two major errors caused by motor delay and arbitrary vibration. In our work, the motor delay was compensated in calibration step by finding appropriate phase delay of FTL signal (-28.75 degrees ≈ 2.8 ms). On the other hand, arbitrary vibration could not be compensated because our system does not have real-time focal length tracker. Although tomographic projector shows convincing reliability of focal plane reconstruction as shown in Figure 6, artificial vibration may cause dioptric error. The study by [Chang et al. 2018] contributes to settle this issue by introduction of feedback circuit. We believe that the error amount is acceptable range in consideration of VAC range, but it should be improved for comfortable viewing experience in commercialization step.

6.4 Magnification and Field of View

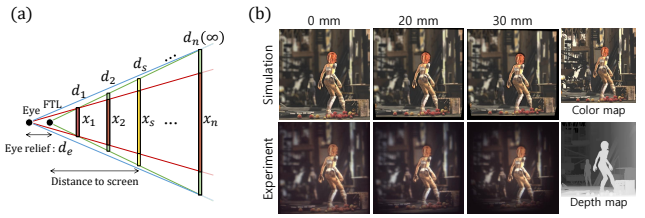

Fig. 17. (a) Illustration of FOV variation according to the depth of focal plane and eye relief. (b) Corresponding simulation and experimental results are demonstrated when the eye relief changes from 0 to 30 mm. The source of 3D contents is from the work of [Butler et al. 2012]

In tomographic projector, users wear the FTL in the form of an eyewear. Eyewear types require eye relief which is the distance between the lens and eye more than 10 mm. Due to the eye relief, the magnification of each depth plane becomes different. As shown in Figure 17 (a), FOV of each focal plane diminishes as the distance gets closer. This can be expressed as

$$FOV_n = 2\tan^{-1}\left(\frac{x_n}{2(d_e + d_n)}\right), \tag{8}$$

where $x_n = (d_n/d_s)x_s$. d_e is the distance of eye relief, d_n is the distance to n-th focal plane, d_s is the distance to the projection screen, x_s is the projection screen size, and x_n is the size of virtual screen image. The upper-bound of FOV is given by

$$FOV_{max} \cong 2\tan^{-1}\frac{x_s}{2d_s}, \tag{9}$$

where the distance from a screen is infinite or the eye relief is zero. The maximum difference of screen size is calculated as below according to the Eq. 8.

$$\Delta Size_{max} = \left(\frac{\%}{100}\right) = \frac{\tan FOV_{max}}{\tan FOV_1} - 1 = \frac{d_e}{d_1} \tag{10}$$

According to the above equation, the defect gets notable when the difference in depths gets wider. Additionally, the defect gets more noticeable as the distance from the center gets larger. In our system, combination of DMD and SLMs increases focal plane number without scarifying bit depth or frame rate. However, this configuration has drawback that is correlation of each focal plane images. Therefore, it is hard to digitally compensate magnification variation of each depth plane. However, in a typical viewing environment, magnification does not cause significant problems. Since the optical axis and gaze direction of a user are identical, less error is observed in fovea. We can also modify optimization algorithm to mitigate the artifacts caused by magnification variation. Moreover, taking retinal blur into consideration, focal blur effect could be strong enough to make the error hardly noticeable where the depth is discontinuous as shown in Figure 17 (b).

7 CONCLUSION

We have presented a tomographic projection system that can be applied to a large screen such as movie theater to give more immersive and comfortable experience. The tomographic projector combines SLMs for color and contrast and DMD for fast spatial filtering, which are synchronized with the focus-tunable lens. In a theater using a tomographic projector, audience perceives the monocular depth information that was not available before. We have implemented a miniaturized environment of theater and confirmed that quasi-continuous focus cues are reconstructed by the tomographic projector. We have thoroughly analyzed the viewing zone where uniform 3D experience is delivered regardless of seat position. According to our analysis, tomographic projector do not cause significant focus cue distortion in the practical environment where projection screen is meters away from viewers. In addition, it has been verified that our projection system could solve some of the limitations that existed in conventional stereoscopic 3D such as various IPD problem and vergence accommodation conflict. To enhance viewing experience, we have proposed an optimization algorithm

to reduce the occlusion boundary artifacts. The artifact mitigation in the occlusion boundary was demonstrated through simulations and experiments. Finally, we have conducted an in-depth discussion about challenges that should be considered for practical use. We believe that the proposed system could provide a new era of immersive viewing experience in 3D theater.

ACKNOWLEDGMENTS

This work is partially supported by the Institute for Information and Communications Technology Promotion Grant funded by the Korea Government (MSIT) (Development of vision assistant HMD and contents for the legally blind and low vision) under Grant 2017-0-00787.

REFERENCES

Kurt Akeley, Simon J Watt, Ahna Reza Girshick, and Martin S Banks. 2004. A stereo display prototype with multiple focal distances. *ACM Trans. Graph.* 23, 3 (2004), 804–813.

Anders H Andersen and Avinash C Kak. 1984. Simultaneous algebraic reconstruction technique (SART): a superior implementation of the ART algorithm. *Ultrasonic imaging* 6, 1 (1984), 81–94.

D. J. Butler, J. Wulff, G. B. Stanley, and M. J. Black. 2012. A naturalistic open source movie for optical flow evaluation. In *European Conf. on Computer Vision (ECCV) (Part IV, LNCS 7577)*, A. Fitzgibbon et al. (Eds.) (Ed.). Springer-Verlag, 611–625.

Jen-Hao Rick Chang, BVK Kumar, and Aswin C Sankaranarayanan. 2018. Towards multifocal displays with dense focal stacks. In *SIGGRAPH Asia 2018 Technical Papers*. ACM, 198.

Heejin Choi, Joohwan Kim, Seong-Woo Cho, Yunhee Kim, Jae Byung Park, and Byoungho Lee. 2008. Three-dimensional-two-dimensional mixed display system using integral imaging with an active pinhole array on a liquid crystal panel. *Applied optics* 47, 13 (2008), 2207–2214.

Suyeon Choi, Seungjae Lee, Youngjin Jo, Dongheon Yoo, Dongyeon Kim, and Byoungho Lee. 2019. Optimal binary representation via non-convex optimization on tomographic displays. *Optics Express* 27, 17 (2019), 24362–24381.

Neil A Dodgson. 2005. Autostereoscopic 3D displays. *Computer* 38, 8 (2005), 31–36.

David Dunn, Cary Tippets, Kent Torell, Petr Kellnhofer, Kaan Akşit, Piotr Didyk, Karol Myszkowski, David Luebke, and Henry Fuchs. 2017. Wide field of view varifocal near-eye display using see-through deformable membrane mirrors. *IEEE Transactions on Visualization and Computer Graphics* 23, 4 (2017), 1322–1331.

Netalee Efrat, Piotr Didyk, Mike Foshey, Wojciech Matusik, and Anat Levin. 2016. Cinema 3D: large scale automultiscopic display. *ACM Transactions on Graphics (TOG)* 35, 4 (2016), 59.

Zhongpai Gao, Alex Hwang, Guangtao Zhai, and Eli Peli. 2018. Correcting geometric distortions in stereoscopic 3D imaging. *PloS one* 13, 10 (2018), e0205032.

Gabor T Herman and Attila Kuba. 2012. *Discrete tomography: Foundations, algorithms, and applications*. Springer Science & Business Media.

Matthew Hirsch, Gordon Wetzstein, and Ramesh Raskar. 2014. A compressive light field projection system. *ACM Transactions on Graphics (TOG)* 33, 4 (2014), 58.

David M Hoffman, Ahna R Girshick, Kurt Akeley, and Martin S Banks. 2008. Vergence–accommodation conflicts hinder visual performance and cause visual fatigue. *Journal of vision* 8, 3 (2008), 33–33.

Fu-Chung Huang, Kevin Chen, and Gordon Wetzstein. 2015. The light field stereoscope: immersive computer graphics via factored near-eye light field displays with focus cues. *ACM Trans. Graph.* 34, 4 (2015), 60.

Haruo Isono, Minoru Yasuda, and Hideaki Sasazawa. 1993. Autostereoscopic 3-D display using LCD-generated parallax barrier. *Electronics and Communications in Japan (Part II: Electronics)* 76, 7 (1993), 77–84.

Changwon Jang, Kiseung Bang, Gang Li, and Byoungho Lee. 2018. Holographic near-eye display with expanded eye-box. In *SIGGRAPH Asia 2018 Technical Papers*. ACM, 195.

Michael Kalloniatis and Charles Luu. 2007. Temporal resolution. (2007).

Yunhee Kim, Joohwan Kim, Jin-Mo Kang, Jae-Hyun Jung, Heejin Choi, and Byoungho Lee. 2007. Point light source integral imaging with improved resolution and viewing angle by the use of electrically movable pinhole array. *Optics Express* 15, 26 (2007), 18253–18267.

R. Konrad, E.A Cooper, and G. Wetzstein. 2016. Novel Optical Configurations for Virtual Reality: Evaluating User Preference and Performance with Focus-tunable and Monovision Near-eye Displays. In *Proc. CHI*. 1211–1220.

Robert Konrad, Nitish Padmanaban, Keenan Molner, Emily A. Cooper, and Gordon Wetzstein. 2017. Accommodation-invariant Computational Near-eye Displays. *ACM Trans. Graph.* 36, 4 (2017), 88.

Frank L Kooi and Alexander Toet. 2004. Visual comfort of binocular and 3D displays. *Displays* 25, 2-3 (2004), 99–108.

Marc TM Lambooij, Wijnand A IJsselsteijn, and Ingrid Heynderickx. 2007. Visual discomfort in stereoscopic displays: a review. In *Stereoscopic Displays and Virtual Reality Systems XIV*, Vol. 6490. International Society for Optics and Photonics, 64900I.

Douglas Lanman, Matthew Hirsch, Yunhee Kim, and Ramesh Raskar. 2010. Content-adaptive parallax barriers: optimizing dual-layer 3D displays using low-rank light field factorization. *ACM Trans. Graph.* 29, 6 (2010), 163.

Douglas Lanman and David Luebke. 2013. Near-eye light field displays. *ACM Transactions on Graphics (TOG)* 32, 6 (2013), 220.

Lewis. Larmore. 1965. *Introduction to photographic principles / Lewis Larmore* (2d ed. ed.). Dover Publications New York. ix, 229 p. pages.

Jungjin Lee, Sangwoo Lee, Younghui Kim, and Junyong Noh. 2016. ScreenX: Public immersive theatres with uniform movie viewing experiences. *IEEE transactions on visualization and computer graphics* 23, 2 (2016), 1124–1138.

Seungjae Lee, Jaebum Cho, Byounghyo Lee, Youngjin Jo, Changwon Jang, Dongyeon Kim, and Byoungho Lee. 2018. Foveated retinal optimization for see-through near-eye multi-layer displays. *IEEE Access* 6 (2018), 2170–2180.

Seungjae Lee, Youngjin Jo, Dongheon Yoo, Jaebum Cho, Dukho Lee, and Byoungho Lee. 2019. Tomographic near-eye displays. *Nature communications* 10, 1 (2019), 2497.

Gang Li, Dukho Lee, Youngmo Jeong, Jaebum Cho, and Byoungho Lee. 2016. Holographic display for see-through augmented reality using mirror-lens holographic optical element. *Opt. Lett.* 41, 11 (2016), 2486–2489.

Gabriel Lippmann. 1908. Epreuves reversibles Photographies integrals. *Comptes-Rendus Academie des Sciences* 146 (1908), 446–451.

Kevin J MacKenzie, David M Hoffman, and Simon J Watt. 2010. Accommodation to multiple-focal-plane displays: Implications for improving stereoscopic displays and for accommodation control. *Journal of Vision* 10, 8 (2010), 22–22.

Andrew Maimone and Henry Fuchs. 2013. Computational augmented reality eyeglasses. In *Proc. ISMAR*. 29–38.

Andrew Maimone, Andreas Georgiou, and Joel S. Kollin. 2017. Holographic Near-Eye Displays for Virtual and Augmented Reality. *ACM Trans. Graph.* 36, 4 (2017), 85.

Michael Mauderer, Simone Conte, Miguel A Nacenta, and Dhanraj Vishwanath. 2014. Depth perception with gaze-contingent depth of field. In *Proceedings of the SIGCHI Conference on Human Factors in Computing Systems*. ACM, 217–226.

Bernard Mendiburu. 2012. *3D movie making: stereoscopic digital cinema from script to screen*. Focal press.

Olivier Mercier, Yusufu Sulai, Kevin Mackenzie, Marina Zannoli, James Hillis, Derek Nowrouzezahrai, and Douglas Lanman. 2017. Fast gaze-contingent optimal decompositions for multifocal displays. *ACM Trans. Graph.* 36, 6 (2017), 237.

Rahul Narain, Rachel A Albert, Abdullah Bulbul, Gregory J Ward, Martin S Banks, and James F O'Brien. 2015. Optimal presentation of imagery with focus cues on multi-plane displays. *ACM Trans. Graph.* 34, 4 (2015), 59.

Yuji Nojiri, Hirokazu Yamanoue, Atsuo Hanazato, Masaki Emoto, and Fumio Okano. 2004. Visual comfort/discomfort and visual fatigue caused by stereoscopic HDTV viewing. In *Stereoscopic Displays and Virtual Reality Systems XI*, Vol. 5291. International Society for Optics and Photonics, 303–314.

Nitish Padmanaban, Robert Konrad, Tal Stramer, Emily A Cooper, and Gordon Wetzstein. 2017. Optimizing virtual reality for all users through gaze-contingent and adaptive focus displays. *Proceedings of the National Academy of Sciences* 114, 9 (2017), 2183–2188.

Jae-Hyeung Park, Keehoon Hong, and Byoungho Lee. 2009. Recent progress in three-dimensional information processing based on integral imaging. *Applied Optics* 48, 34 (2009), H77–H94.

Soon-gi Park, Jiwoon Yeom, Youngmo Jeong, Ni Chen, Jong-Young Hong, and Byoungho Lee. 2014. Recent issues on integral imaging and its applications. *Journal of Information Display* 15, 1 (2014), 37–46.

Archibald Stanley Percival. 1892. The relation of convergence to accommodation and its practical bearing. *Ophthal. Rev.* 11 (1892), 313–328.

Tom Peterka, Robert L Kooima, Daniel J Sandin, Andrew Johnson, Jason Leigh, and Thomas A DeFanti. 2008. Advances in the dynallax solid-state dynamic parallax barrier autostereoscopic visualization display system. *IEEE transactions on visualization and computer graphics* 14, 3 (2008), 487–499.

Kishore Rathinavel, Hanpeng Wang, Alex Blate, and Henry Fuchs. 2018. An extended depth-at-field volumetric near-eye augmented reality display. *IEEE transactions on visualization and computer graphics* 24, 11 (2018), 2857–2866.

Takashi Shibata, Joohwan Kim, David M Hoffman, and Martin S Banks. 2011. The zone of comfort: Predicting visual discomfort with stereo displays. *Journal of vision* 11, 8 (2011), 11–11.

RE Stevens, DP Rhodes, A Hasnain, and P-Y Laffont. 2018. Varifocal technologies providing prescription and VAC mitigation in HMDs using Alvarez lenses. In *Digital Optics for Immersive Displays*, Vol. 10676. International Society for Optics and Photonics, 106760J.

Yasuhiro Takaki and Nichiyo Nago. 2010. Multi-projection of lenticular displays to construct a 256-view super multi-view display. *Optics express* 18, 9 (2010), 8824–8835.

Kazuhiko Ukai and Peter A Howarth. 2008. Visual fatigue caused by viewing stereoscopic motion images: Background, theories, and observations. *Displays* 29, 2 (2008), 106–116.

Marc von Waldkirch, Paul Lukowicz, and Gerhard Tröster. 2003. Defocusing simulations on a retinal scanning display for quasi accommodation-free viewing. *Optics express* 11, 24 (2003), 3220–3233.

Koki Wakunami, Po-Yuan Hsieh, Ryutaro Oi, Takanori Senoh, Hisayuki Sasaki, Yasuyuki Ichihashi, Makoto Okui, Yi-Pai Huang, and Kenji Yamamoto. 2016. Projection-type see-through holographic three-dimensional display. *Nature communications* 7 (2016), 12954.

Gordon Wetzstein, Douglas Lanman, Wolfgang Heidrich, and Ramesh Raskar. 2011. Layered 3D: tomographic image synthesis for attenuation-based light field and high dynamic range displays. *ACM Trans. Graph.* 30, 4 (2011), 95.

Lei Xiao, Anton Kaplanyan, Alexander Fix, Matthew Chapman, and Douglas Lanman. 2018. DeepFocus: learned image synthesis for computational displays. In *SIGGRAPH Asia 2018 Technical Papers*. ACM, 200.